Original Article

Beam Characterization of 10-MV Photon Beam from Medical Linear Accelerator without Flattening Filter

Tomohiro Shimozato, Yuichi Aoyama[1], Takuma Matsunaga[2], Katsuyoshi Tabushi[3]

Department of Radiological Technology, School of Health Sciences, Gifu University of Medical Science, Seki, Gifu, [1]Department of Radiation Oncology, Kobe University Hospital, Kobe, Hyougo, [2]Department of Radiology, Seirei Hamamatsu General Hospital, Hamamatsu, Shizuoka, [3]Department of Radiological Technology, Nagoya University Graduate School of Medicine, Nagoya, Aichi, Japan

Abstract

Aim: This work investigated the dosimetric properties of a 10-MV photon beam emitted from a medical linear accelerator (linac) with no flattening filter (FF). The aim of this study is to analyze the radiation fluence and energy emitted from the flattening filter free (FFF) linac using Monte Carlo (MC) simulations. **Materials and Methods:** The FFF linac was created by removing the FF from a linac in clinical use. Measurements of the depth dose (DD) and the off-axis profile were performed using a three-dimensional water phantom with an ionization chamber. A MC simulation for a 10-MV photon beam from this FFF linac was performed using the BEAMnrc code. **Results:** The off-axis profiles for the FFF linac exhibited a chevron-like distribution, and the dose outside the irradiation field was found to be lower for the FFF linac than for a linac with an FF (FF linac). The DD curves for the FFF linac included many contaminant electrons in the build-up region. **Conclusion:** Therefore, for clinical use, a metal filter is additionally required to reduce the effects of the electron contamination. The mean energy of the FFF linac was found to be lower than that of the FF linac owing to the absence of beam hardening caused by the FF.

Keywords: External radiotherapy, flattening filter, high-energy photon beam, Monte Carlo simulation

Received on: 13-07-2016 **Review completed on: 25-02-2017** **Accepted on: 02-03-2017**

Introduction

To create a uniform photon field from a general medical linear accelerator (linac) for the external irradiation of the human body, it is standard practice to follow the photon-emitting metal target with a conical metal flattening filter (FF) inserted into the beam's path. Although a uniform distribution within the irradiated area may be obtained, the dose rate gets reduced because of attenuation. To mitigate this, flattening filter free (FFF) linacs have been developed recently. As the name implies, they have no FF and instead utilize bremsstrahlung radiation emitted directly from the target. Such devices are currently used in clinical applications.[1,2]

The dose distribution for FFF linacs determined using Monte Carlo (MC) simulations,[3-11] as well as measured data from treatment apparatuses in clinical use,[8-18] has been published. Most of such experimental studies employed commercial linacs with a metal plate, such as copper or aluminum, inserted to absorb the primary and secondary electrons created in materials in the linac head.

Access this article online

Quick Response Code:

Website: www.jmp.org.in

DOI: 10.4103/jmp.JMP_71_16

Vassiliev *et al*.[10,15] reported that removing the FF from a Varian-type linac changed the output factor (total scatter factor) and dose distribution for 6- and 18-MV photon beams. They reported that the changes in the output factor for FFF linac were smaller than those for FF linac and that the surface dose for the FFF linac was larger than that for the FF linac. However, the distribution of the electron beam generated from the target, monitor chamber, mirror, jaws, and other structures – which contributes significantly to the buildup area of the depth dose (DD) curves for a 10-MV photon beam in FFF – has hardly been reported.[12,16,17]

Kragl *et al*.[16] reported the dosimetric characteristics of 6- and 10-MV unflattened photon beams by precisely controlling a

Address for correspondence: Dr. Tomohiro Shimozato, Department of Radiological Technology, School of Health Sciences, Gifu University of Medical Science, 795-1, Nagamine Ichihiraga, Seki, Gifu, Japan.
E-mail: shimo-p@umin.ac.jp

How to cite this article: Shimozato T, Aoyama Y, Matsunaga T, Tabushi K. Beam characterization of 10-MV photon beam from medical linear accelerator without flattening filter. J Med Phys 2017;42:65-71.

commercial linac manufactured by Elekta, equipped with a metal filter for the elimination of contamination electrons. Wang *et al*. investigated the surface dose under 6- and 10-MV photon beams generated by a Varian TrueBeam linac. FFF linacs equipped with metal filters have also been investigated for the elimination of contamination electrons.[19,20] The electron contamination due to the relationship between the energy and the thickness of the target is expected in the case of 10-MV photon beams.

This work investigated the beam characteristics of an FFF linac to measure data such as the DD and off-axis profiles, and fluence distribution calculated by an MC simulation of a 10-MV FFF photon beam. Furthermore, using the BEAMnrc MC code provided by the National Research Council, Canada (NRCC), this work investigated the effects of the FF on the dose distribution. In the present study, we obtained this data and performed a radiation component analysis through MC simulations. This study investigated the changes in the fluence and energy using the BEAMDP software (provided by NRCC)[21] to analyze the phase space data (PSD) and clarify the difference between the photon beam fluence distributions emitted from the FF and FFF linacs.

Materials and Methods

Measurement of depth ionization and off-axis profile

The measurements were conducted on a Varian Clinac 2100CD (Varian Medical Systems, Palo Alto, CA, USA). To create the FFF linac, the FF was removed from the carousel that the FF is typically installed on. The FFF linac was then operated in "service mode," with several hardware and software interlocks overridden, mainly to allow for the beam delivery and control the dose by servo. By measuring the head scatter factor in air in the direction of the off-axis, it was confirmed that the photon beam passed through the FF perpendicularly when the dose servo was off. The depth-ionization curves and the off-axis profiles used to determine off-axis ratio characteristics in water were measured using a three-dimensional (3D) water phantom (PTW MP3 water tank, PTW-Freiburg, Germany). A 10-MV photon beam was emitted from the linac.

The depth-ionization curves and the off-axis profiles were acquired with a water phantom using a type-31010 SemiFlex thimble ionization chamber with a volume of 0.125 cm^3 (PTW-Freiburg, Germany). The depth-ionization curves were obtained at a 100-cm source-to-surface distance (SSD) for square field sizes of 5 cm × 5 cm, 10 cm × 10 cm, 20 cm × 20 cm, and 30 cm × 30 cm determined by jaws using a step size of 0.1 cm with the water tank controlled by the MEPHYSTO software (PTW-Freiburg, Germany). The scanning data were acquired following the recommendations given in Task Group (TG)-106.[22] The depth-ionization curves were then measured by moving the ionization chamber from depth to surface. Their curves were normalized to the dose value measured at a depth of 10 cm.

The off-axis profiles were then measured at 0.7, 5, and 10 cm depths for each field size. The special measurement depth of 0.7 cm corresponded to the peak depth of contamination electrons in the buildup region obtained through the depth-ionization curves, as discussed later. The step size of the off-axis profile was 1 mm for each field size. The off-axis profiles were measured in the cross-plane (transverse direction) and normalized to the dose at the central axis of the beam. Only cross-plane profiles are reported here as measurements showed that the difference between cross-plane and in-plane profiles was considered negligible. Because the radiation fluence in the shallow region may include many primary and secondary electrons in the photon beam, the effect of the stopping-power ratio (SPR) for the electron beam cannot be neglected.[23] In the case of the photon beam, given that the change in the SPR with the depth is small, a comparison is often made with the MC by replacing the percentage DD (PDD) with percentage depth ionization (PDI). For the electron beam, although the difference between the PDI and PDD in the buildup region with 4–8 MeV was about 3%,[22] it can be compared to the MC for the off-axis profile using irradiation curves that have not been converted by SPR. This work did not consider the SPR for significantly electron-contaminated photon beams.

Monte Carlo simulation

The BEAMnrc MC simulation code,[24,25] which is based on the EGSnrc coupled photon-electron transport code,[26] was used to model the linac treatment head according to the manufacturer's specifications. The linac in the BEAMnrc MC simulation configures parts such as the bremsstrahlung target, primary collimator, beryllium window, FF, monitor chamber, mirror, movable collimators (X and Y jaws), and multileaf collimator (MLC).[27] In the Varian linac, the target was made of copper for a 10-MV photon beam. The FFs and the electron-scatter foils are mounted on a rotating circular metallic carousel. In this study, the metallic carousel body was not included in the simulation. The FF for a 10-MV photon beam was cone-shaped and made of copper. The jaws and MLC were made of tungsten. The driving motor and the substrate lead blocks for preventing leakage were not reproduced in the MC simulation. It is assumed that the radiation scattered from these parts was absorbed by the jaws downstream and had limited influence on the simulation results.

To determine the parameters of the linac constructed on BEAMnrc, the DD curves and the off-axis profiles calculated by the MC simulation were compared with the measured values of DD curves and off-axis profiles for an unaltered linac equipped with an FF. PSD calculated using the BEAMnrc MC code were recorded at an SSD of 100 cm. Variance-reduction processing techniques, such as forcibly increasing the number of photons, were not used in our study. The ratios of the electron to the photon fluence were a significant factor in this work, and applying a variance-reduction technique such as forcibly increasing the number of photons may change these ratios.

The dose in the water phantom was calculated from the PSD output from the BEAMnrc simulation using the EGSnrc/DOSXYZnrc code.[28] Transport parameters of AE = ECUT = 0.521 MeV and AP = PCUT = 0.01 MeV

were selected, and the fractional energy loss per electron step (ESTEPE) was controlled by the PRESTA-II electron-step transport algorithm. The electron range rejection method was not used. The PSD were then used as an input to compute the dose distributions in the water phantom, using the DOSXYZnrc code for 3D absorbed dose calculations in Cartesian coordinates. The size of the water phantom was 40 cm × 40 cm × 40 cm, and its front surface was placed on the same plane as the isocenter (100-cm SSD).

The treatment head model configured in the BEAMnrc code was validated by comparing the measured and DOSXYZnrc-calculated DD curves and off-axis profiles in the cross-plane. This work compared the MC simulation values with the measured values for the DD curves normalized to a dose at a depth of 10 cm. The differences between the measured and calculated data were considered as the ratio of calculated data to the measured data. The simulations were performed in ten batches, and the statistical uncertainty, estimated as one standard deviation, was maintained below 1% inside the primary radiation field, except in the DD curve buildup and off-axis profile penumbra regions. According to AAPM TG-105,[29] the MC modeling of the linac head is not recommended for analyzing the statistical uncertainty clearly. A statistical uncertainty of ±1% was used in the estimation by the MC simulation code. Then, the difference between the data calculated from the MC simulation and the measured data was evaluated at 1%–2%. The difference in the buildup region of the DD curves was evaluated as being within 3%. Thus, the differences in the penumbra regions of the off-axis profiles were evaluated as being no more than 3%.

The simulation was performed in Microsoft Windows XP SP2 with the g77 compiler installed on a system with an Intel Core™2 Duo E6850 3.0 GHz processor having 2.0 GB of RAM. The number of primary electrons was approximately 400 million for the BEAMnrc simulation. For the DOSXYZnrc simulation, the number of histories was 5000 million. The material library Preprocessor for EGS4 (PEGS4) data file was used; those material properties that did not appear by default in PEGS4 were determined using the EGSnrc multiplatform (EGSnrcMP)[30] and thereafter added to the simulation. The mean energy of the initial primary electrons and the initial electron beam source spread was determined by finding the best fit between the MC model and the measured DDs and off-axis profiles.

The source was simulated as a Gaussian energy distribution by setting ISOURCE = 19. The energies of the incident electrons used in the MC simulation were determined by matching the measured values obtained using the ionization chamber to those calculated by the MC simulation. The incident energy in MC simulations was adjusted as the slope beyond d_{max} (depth at maximum dose) of the calculated DD curves approached the measured curves.

DD-curve and the off-axis profile dose calculations for the FFF linac were performed using DOSXYZnrc to input the PSD calculated for the removed FF using BEAMnrc. The calculated dose curves were plotted using STATDOSE.[31] The fluence and energy were analyzed using the BEAMDP software[20] with the PSD obtained using the BEAMnrc code.

Results and Discussion

Comparison between measured and calculated depth dose curves and off-axis profiles of the flattening filter linac

Figure 1a shows a comparison between the measured depth-ionization curves using an ionization chamber and the MC simulation for square jaw-defined field sizes of side length 5, 10, 20, and 30 cm. Figure 1b shows the measured off-axis profiles and the calculated values of the MC simulation for square jaw-defined field sizes of side length 5, 10, 20, and 30 cm at a depth of 10 cm. The best fit of the MC model to the measured DDs and off-axis profiles was with an initial mean primary electron energy of 10.3 MeV and a Gaussian energy spread with FWHM of 3.12 MeV and the electron beam source spread of a Gaussian spatial distribution with a FWHM of 1.8 mm.

The difference between the measured and calculated values was within 1% beyond the depth of maximum dose, and the difference in the buildup region was within 7%/2 mm. The

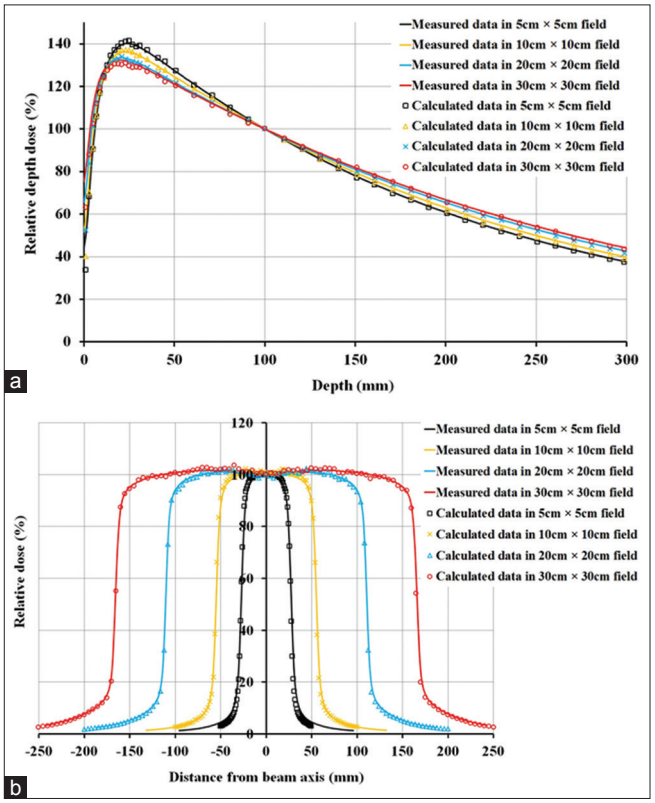

Figure 1: Depth-ionization curves and off-axis profiles measured in the ionization chamber and depth dose curves calculated using a Monte Carlo simulation of the flattening filter linac. (a) Depth curves for the 5 cm × 5 cm, 10 cm × 10 cm, 20 cm × 20 cm, and 30 cm × 30 cm fields, (b) off-axis profiles at 10 cm depth in the respective fields.

difference in the off-axis profile was within 1% in all regions except for the penumbra, and the difference in penumbra region was within 5%/1 mm. The penumbra was defined as the region between 1 cm inside the field edge and 2 cm outside the field edge, according to the definition indicated by ESTRO Booklet No. 7.[32]

The surface dose and buildup region in the photon beam are associated with the complex behavior of electron contamination. The readout values in this region differ according to the type of detector used.[22] According to Das *et al*.,[22] the SPR necessary to convert the depth-ionization curves to DD curves differs from ~ 3% to d_{max} from the surface for 4- and 8-MeV electron beams. For a photon beam, a change in the depth yields a small change in the SPR. The conversion of the depth ionization to the DD was not performed for the data obtained by the scanning measurement.

Comparison of measured and calculated depth dose curves of the flattening filter free linac

The MC simulation of the FFF linac was created by removing the FF and using the BEAMnrc parameters previously determined in this work. The DD curve and off-axis profile of the FFF linac were calculated using DOSXYZnrc on the calculated PSD in BEAMnrc. A comparison of the DD curves and profiles calculated by the MC simulation to those directly measured was performed for a 10-MV photon beam emitted from the FFF linac.

The DD curves were normalized to the corresponding values obtained from the respective curve at a depth of 10 cm. Because the DD curves calculated by the MC simulation have statistical noise, normalizing at d_{max} may disproportionately affect the shape of the DD curve beyond d_{max}. The difference between the values calculated using the MC simulation and the measured data were <0.5% beyond d_{max} for fields of 5 cm × 5 cm, 10 cm × 10 cm, 20 cm × 20 cm, and 30 cm × 30 cm, as shown in Figure 2. For the buildup region, the DD curves of the FFF linac exhibited rapid dose changes. The dose percentage in the buildup region increased with the size of the irradiation field. As shown in Figure 2, the DD curves in the FFF linac differed noticeably from those of the FF linac. At a depth corresponding to the buildup region of the FF linac, the FFF linac exhibited a DD distribution with a sharp pointed curve. As shown in Figure 2, the DD curves calculated from the MC simulation and those measured in the ionization chamber for the FFF linac exhibited a similar trend. As indicated by the sharp spike at shallow depth, there was evidence for electron beam contamination that interacted with the target, primary collimator, and monitor chamber. The energy of the photon beam emitted from the FFF linac was lower than that of the beam from the FF linac because the PDD slope of the FFF linac is smaller than that of the FF linac.

Figure 3 shows the radiation fluences of the FFF and FF linacs calculated using the BEAMDP software for the PSD analysis. As shown in Figure 3a, the photon fluence from the FFF linac was not attenuated by the FF and therefore was greater than that from the FF linac. It may thus be considered that the radiation fluence of the FFF linac contained many

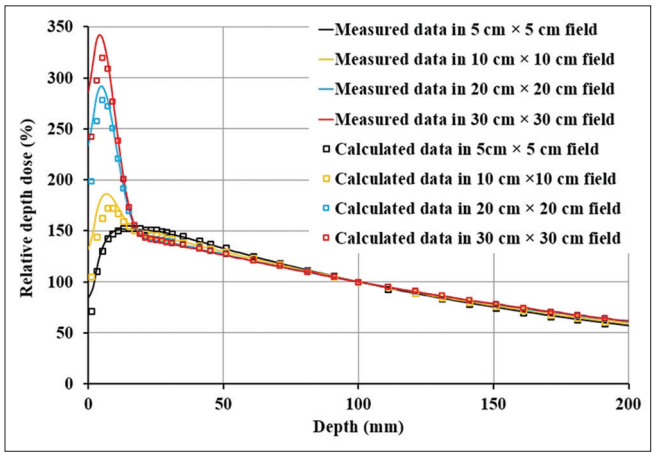

Figure 2: Depth-ionization curves measured in the ionization chamber and depth dose curves calculated using a Monte Carlo simulation of the flattening filter free linac. The depth curves are for the 5 cm × 5 cm, 10 cm × 10 cm, 20 cm × 20 cm, and 30 cm × 30 cm fields.

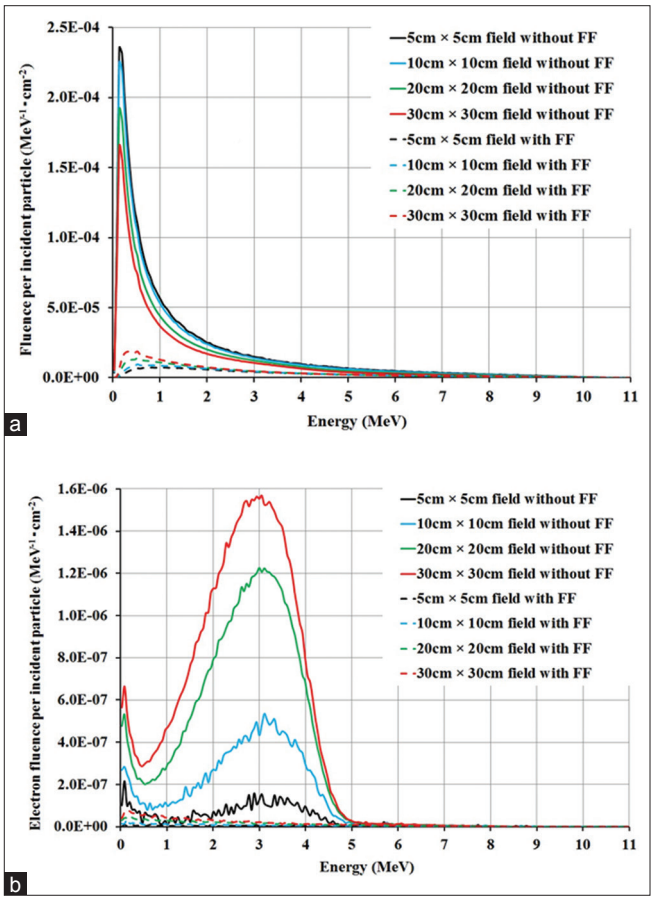

Figure 3: Fluence distributions for radiation emitted from the flattening filter and flattening filter free linacs in 5 cm × 5 cm, 10 cm × 10 cm, 20 cm × 20 cm, and 30 cm × 30 cm fields. (a) Photon fluence and (b) electron fluence.

low-energy components that were not absorbed by the metallic FF. Furthermore, the electron beam contribution increased rapidly as the exposure field increased in the FFF linac, as shown in Figure 3b. The contamination electrons contributed to a rapid dose escalation in the buildup region of the depth-ionization curve, as shown in Figure 2. The mean contamination electron energies for the FF linac were 2.65, 2.59, 2.31, and 2.09 MeV for the 5 cm × 5 cm, 10 cm × 10 cm, 20 cm × 20 cm, and 30 cm × 30 cm fields, respectively. Those for the FFF linac were 2.58, 2.72, 2.66, and 2.59 MeV for the 5 cm × 5 cm, 10 cm × 10 cm, 20 cm × 20 cm, and 30 cm × 30 cm fields, respectively. The integrations of the electron fluence of the FFF linac were 27.0, 23.8, 27.5, and 26.5 times those of the FF linac for the 5 cm × 5 cm, 10 cm × 10 cm, 20 cm × 20 cm, and 30 cm × 30 cm fields, respectively.d It is considered that the mean energy and fluence are not proportional to the irradiation field, and these relate the distances and the position relations between the target and secondary collimators. The integrations of the photon fluence of the FFF linac were 7.4, 6.2, 4.5, and 3.4 times those of the FF linac for the 5 cm × 5 cm, 10 cm × 10 cm, 20 cm × 20 cm, and 30 cm × 30 cm fields, respectively. Thus, the reductions in electron contamination fluence and photon fluence suggest that the FF strongly contributes to absorption of contamination electrons and photon attenuation.

Comparison of measured and calculated off-axis profile of flattening filter free linac

The off-axis profiles obtained by the MC simulation and measured using the ionization chamber for the 10-MV output photon beam of the FFF linac are shown in Figure 4. This figure provides the calculated and measured off-axis profiles for the 5 cm × 5 cm, 10 cm × 10 cm, 20 cm × 20 cm, and 30 cm × 30 cm fields. The depths shown in Figure 4 are 0.7, 5, and 10 cm in the respective irradiation fields, and the off-axis profiles are normalized to the appropriate values at the beam center axis for the respective irradiation fields. As shown in Figure 4b and c, the off-axis profiles have convex distributions that agree with the literature.[3,10,13,15,16,18-20] The profile in the off-axis direction at the 0.7-cm depth, where many contamination electrons are contained, differs from the profiles at deeper positions under the influence of entrained electrons. This is because the electron beam spreads laterally after entering water and is larger than X-rays, as shown in Figure 4a.

Figure 5 shows the calculation results from the MC simulation of the off-axis profile for the FFF and FF linacs at a depth of 10 cm for the 5 cm × 5 cm, 10 cm × 10 cm, 20 cm × 20 cm, and 30 cm × 30 cm fields. It can be seen that the difference between the off-axis profiles of FF and FFF increases with increasing distance from the central beam axis when the field size increases. A comparison

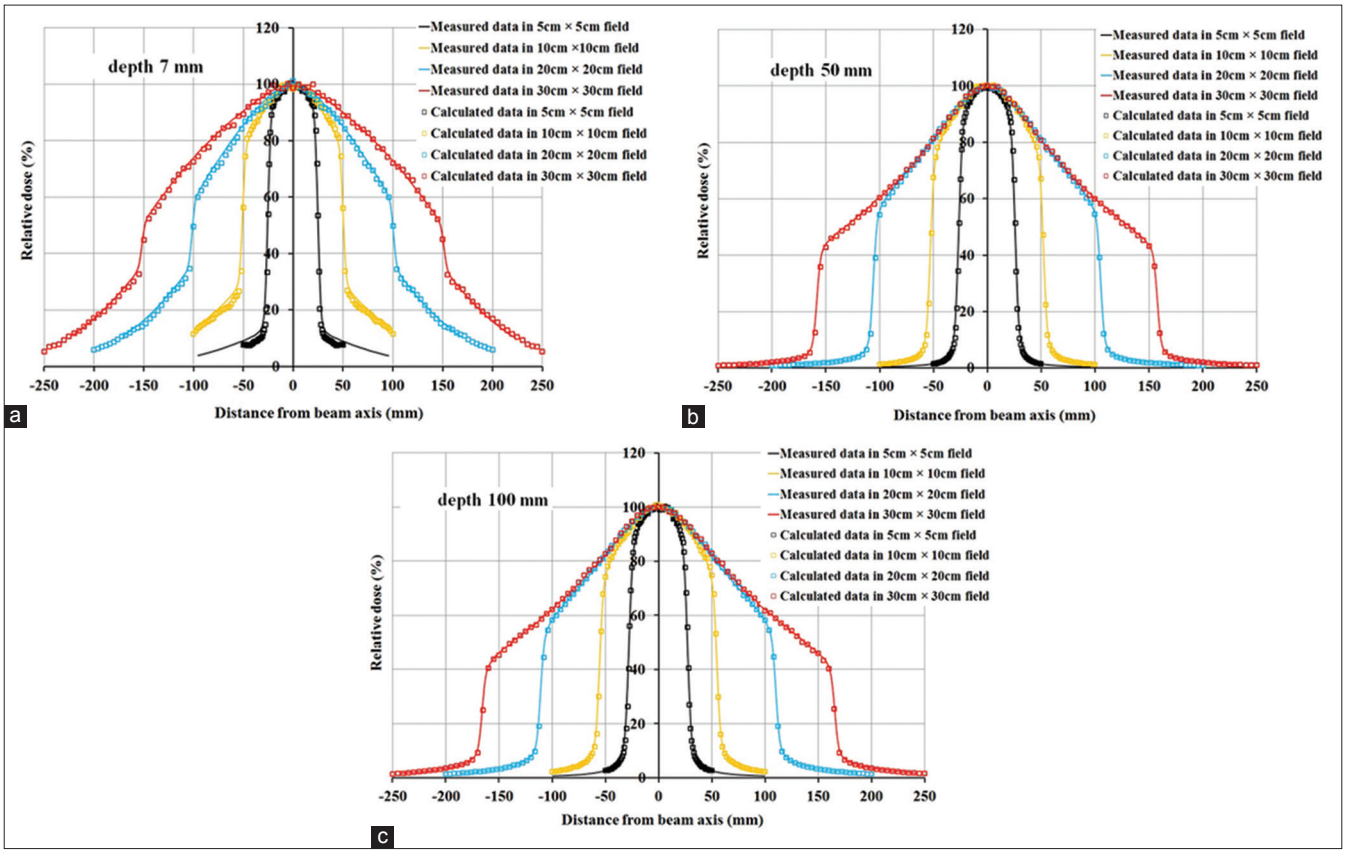

Figure 4: Off-axis profiles measured in the ionization chamber and calculated using a Monte Carlo simulation of the flattening filter free linac. Off-axis profiles in the respective fields (a) at 0.7 cm depth, (b) at 5 cm depth, and (c) at 10 cm depth.

of the values 1 cm inside the edge and 2 cm outside the radiation field for the off-axis profiles of the FF and FFF linacs, normalized to the value of the central beam axis in the respective irradiation fields, is provided in Table 1. The ratios shown in Table 1 were calculated as FFF/FF. At depths of 5 and 10 cm, the ratios of the off-axis profile values of the FFF linac to those of the FF linac were smaller than 1.00 at 1 cm inside the field edge (the minimum is 0.47 for 30 cm × 30 cm) and 2 cm outside the field edge (the minimum is 0.42 for 30 cm × 30 cm). The dose 1 cm inside the field edge for the FFF linac was lower than that for the FF linac when the field size was larger. The dose 2 cm outside the field edge was also lower than that for the FF linac when the field size was larger. The dose outside the field edge at a depth of 0.7 cm was higher than that of the FF linac because primary and secondary electron beams not absorbed by the FF were scattered.

At a depth of 0.7 cm in the 10 cm × 10 cm irradiation field, the ratio of off-axis profile of the FFF linac to the FF linac 2 cm outside the field edge was 3.22. Because the FF was absent, many electron components were observed in the buildup region at a depth of 0.7 cm, as shown in Figure 2. This is explained by the increase in the dose outside the edge of the irradiation field due to the spreading of the electron beam in the irradiation field. With the dose normalized to the central beam axis, the relative dose in the FFF linac was observed to be lower than that of the FF linac outside the irradiation field. The mean photon energies for the FF linac were 3.01, 2.83, 2.53, and 2.26 MeV for the 5 cm × 5 cm, 10 cm × 10 cm, 20 cm × 20 cm, and 30 cm × 30 cm fields, respectively. Those for the FFF linac were 1.61, 1.59, 1.56, and 1.52 MeV for the 5 cm × 5 cm, 10 cm × 10 cm, 20 cm × 20 cm, and 30 cm × 30 cm fields, respectively. Because the photon energy of the FFF linac was lower than that of an FF linac, the FFF DD tended to be lower than that of the FF beam.

Therefore, the FF was found to attenuate the contamination electrons, and the resulting fluence quantities were lower than that for the FFF beam owing to the spread of the electrons. The study of FFF linac included contamination electrons. These contamination electrons are unnecessary for clinical use because they cause an increase in wasteful skin dose; therefore, the electrons must be removed. Although the type of material leaves room for consideration, it is necessary to insert a thin metal (copper or aluminum) plate into the apparatus to eliminate electron contamination. Figure 6 shows the DD curve when a 2-mm copper filter or a 5-mm aluminum filter is inserted for reference. Although it is necessary to study the material and thickness of the metal, it is possible to reduce the contamination electrons by the copper plate and the aluminum plate.

Table 1: Ratio of the off-axis-ratio values of the FFF linac to the corresponding values for the FF linac

Field size	Depth (cm)	Field edge – 1 cm	Field edge + 2 cm
5 cm × 5cm	0.7	0.94	2.04
	5.0	0.97	0.77
	10.0	0.97	0.87
10 cm × 10 cm	0.7	0.86	3.22
	5.0	0.84	0.68
	10.0	0.85	0.81
20 cm × 20 cm	0.7	0.60	2.50
	5.0	0.61	0.52
	10.0	0.64	0.61
30 cm × 30 cm	0.7	0.52	1.99
	5.0	0.47	0.42
	10.0	0.51	0.46

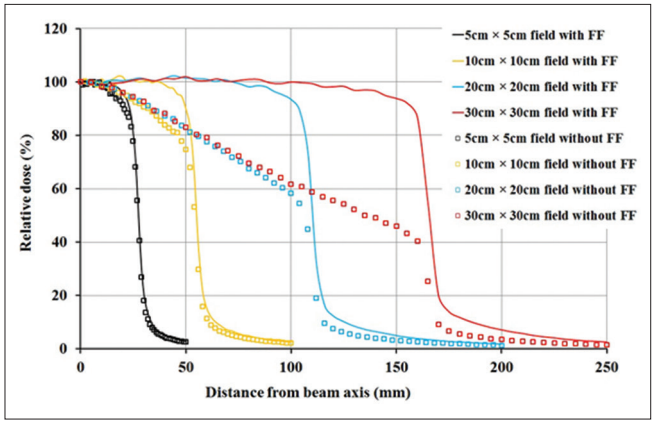

Figure 5: Off-axis profiles at 10 cm depth in the respective fields calculated using Monte Carlo simulations for the flattening filter and flattening filter free linacs.

Conclusions

Dose distributions of an FFF linac and FF linac were studied using MC simulations. To create an FFF linac from an FF

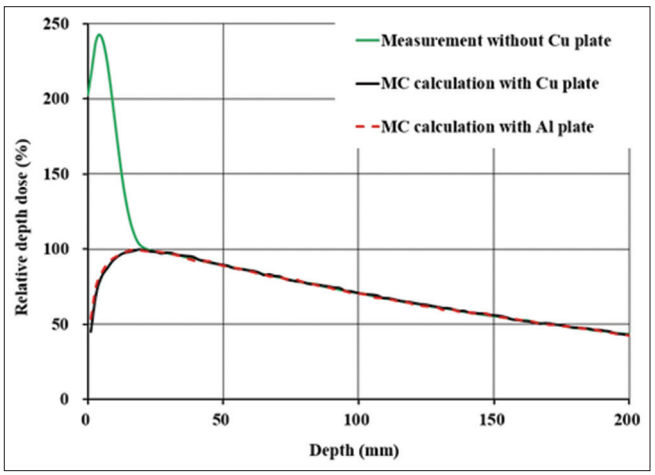

Figure 6: The depth dose curves for radiation emitted from flattening filter free linac measured and calculated by Monte Carlo simulation in 30 cm × 30 cm field. Green line shows the measured depth dose for 10 MV flattening filter free beam without metal filter. Black line shows that with 2 mm thick copper filter. Red dash line shows that with 5 mm thick aluminum filter.

linac, the FF alone was removed. This simulation enabled us to observe changes in the radiation quality due to the lack of an FF. In addition, it was determined that the FF absorbed the electron contamination inside the target. In our study, therefore, it is shown that in designing an FFF linac, it is beneficial to have knowledge about the electron components in the beam, which can be obtained through MC simulations. The insertion of the FF was found to result in not only flattening of the radiation beam but also reduction of the wasteful contamination electrons. A possible extension of this work is determining – through such a simulation – the required type, thickness, etc., of a thin metal plate that can be used to reduce the electron beam contamination. It was found that the dose outside the irradiation field was lower than that in the FF linac because of the reduction of radiation scatter, such as that caused by an FF. It was determined that the mean energy of the FFF linac was lower than that of the FF linac because the photon beams were not affected by the beam hardening typically caused by an FF.

Financial support and sponsorship

Nil.

Conflicts of interest

There are no conflicts of interest.

References

1. Mancosu P, Castiglioni S, Reggiori G, Catalano M, Alongi F, Pellegrini C, *et al.* Stereotactic body radiation therapy for liver tumours using flattening filter free beam: Dosimetric and technical considerations. Radiat Oncol 2012;7:16.
2. Scorsetti M, Alongi F, Castiglioni S, Clivio A, Fogliata A, Lobefalo F, *et al.* Feasibility and early clinical assessment of flattening filter free (FFF) based stereotactic body radiotherapy (SBRT) treatments. Radiat Oncol 2011;6:113.
3. Cashmore J, Golubev S, Dumont JL, Sikora M, Alber M, Ramtohul M. Validation of a virtual source model for Monte Carlo dose calculations of a flattening filter free linac. Med Phys 2012;39:3262-9.
4. Mesbahi A. Dosimetric characteristics of unflattened 6 MV photon beams of a clinical linear accelerator: A Monte Carlo study. Appl Radiat Isot 2007;65:1029-36.
5. Mesbahi A, Mehnati P, Keshtkar A, Farajollahi A. Dosimetric properties of a flattening filter-free 6-MV photon beam: A Monte Carlo study. Radiat Med 2007;25:315-24.
6. Mesbahi A, Nejad FS. Monte Carlo study on a flattening filter-free 18-MV photon beam of a medical linear accelerator. Radiat Med 2008;26:331-6.
7. Parsai EI, Pearson D, Kvale T. Consequences of removing the flattening filter from linear accelerators in generating high dose rate photon beams for clinical applications: A Monte Carlo study verified by measurement. Nucl Instrum Methods Phys Res B 2007;261:755-9.
8. Titt U, Vassiliev ON, Pönisch F, Dong L, Liu H, Mohan R. A flattening filter free photon treatment concept evaluation with Monte Carlo. Med Phys 2006;33:1595-602.
9. Titt U, Vassiliev ON, Pönisch F, Kry SF, Mohan R. Monte Carlo study of backscatter in a flattening filter free clinical accelerator. Med Phys 2006;33:3270-3.
10. Vassiliev ON, Titt U, Kry SF, Pönisch F, Gillin MT, Mohan R. Monte Carlo study of photon fields from a flattening filter-free clinical accelerator. Med Phys 2006;33:820-7.
11. Cashmore J. The characterization of unflattened photon beams from a 6 MV linear accelerator. Phys Med Biol 2008;53:1933-46.
12. Dalaryd M, Kragl G, Ceberg C, Georg D, McClean B, af Wetterstedt S, *et al.* A Monte Carlo study of a flattening filter-free linear accelerator verified with measurements. Phys Med Biol 2010;55:7333-44.
13. Dzierma Y, Licht N, Nuesken F, Ruebe C. Beam properties and stability of a flattening-filter free 7 MV beam-an overview. Med Phys 2012;39:2595-602.
14. Stevens SW, Rosser KE, Bedford JL. A 4 MV flattening filter-free beam: Commissioning and application to conformal therapy and volumetric modulated arc therapy. Phys Med Biol 2011;56:3809-24.
15. Vassiliev ON, Titt U, Pönisch F, Kry SF, Mohan R, Gillin MT. Dosimetric properties of photon beams from a flattening filter free clinical accelerator. Phys Med Biol 2006;51:1907-17.
16. Kragl G, af Wetterstedt S, Knäusl B, Lind M, McCavana P, Knöös T, *et al.* Dosimetric characteristics of 6 and 10MV unflattened photon beams. Radiother Oncol 2009;93:141-6.
17. Wang Y, Khan MK, Ting JY, Easterling SB. Surface dose investigation of the flattening filter-free photon beams. Int J Radiat Oncol Biol Phys 2012;83:e281-5.
18. Cho W, Kielar KN, Mok E, Xing L, Park JH, Jung WG, *et al.* Multisource modeling of flattening filter free (FFF) beam and the optimization of model parameters. Med Phys 2011;38:1931-42.
19. Georg D, Knöös T, McClean B. Current status and future perspective of flattening filter free photon beams. Med Phys 2011;38:1280-93.
20. Hrbacek J, Lang S, Klöck S. Commissioning of photon beams of a flattening filter-free linear accelerator and the accuracy of beam modeling using an anisotropic analytical algorithm. Int J Radiat Oncol Biol Phys 2011;80:1228-37.
21. Ma CM, Rogers DW. BEAMDP as a General-Purpose Utility. Ionizing Radiation Standards, National Research Council of Canada, NRCC Report PIRS-0509(E)revA, 2009.
22. Das IJ, Cheng CW, Watts RJ, Ahnesjö A, Gibbons J, Li XA, *et al.* Accelerator beam data commissioning equipment and procedures: Report of the TG-106 of the Therapy Physics Committee of the AAPM. Med Phys 2008;35:4186-215.
23. Bailey M, Shipley DR, Manning JW. Roos and NACP-02 ion chamber perturbations and water-air stopping-power ratios for clinical electron beams for energies from 4 to 22 MeV. Phys Med Biol 2015;60:1087-105.
24. Rogers DW, Faddegon BA, Ding GX, Ma CM, We J, Mackie TR. BEAM: A Monte Carlo code to simulate radiotherapy treatment units. Med Phys 1995;22:503-24.
25. Rogers DW, Walters B, Kawrakow I. BEAMnrc User's Manual. Ionizing Radiation Standards, National Research Council of Canada, NRCC Report PIRS-0509(A)revK, 2009.
26. Kawrakow I, Rogers DW. The EGSnrc Code System: Monte Carlo Simulation of Electron and Photon Transport. Ionizing Radiation Standards, National Research Council of Canada, NRCC Report PIRS-701, 2000.
27. Varian Medical Systems. Monte Carlo Package High Energy Accelerator. Varian Medical Systems, Serial No. 373, 2008.
28. Wlters B, Kawrakow I, Rogers DW. DOSXYZnrc User's Manual. Ionizing Radiation Standards, National Research Council of Canada, NRCC Report PIRS-794revB, 2009.
29. Chetty IJ, Curran B, Cygler JE, DeMarco JJ, Ezzell G, Faddegon BA, *et al*. Report of the AAPM Task Group No 105: Issues associated with clinical implementation of Monte Carlo-based photon and electron external beam treatment planning. Med Phys 2007;34:4818-53.
30. Kawrakow I, Mainegra-Hing E, Rogers DW. EGSnrcMP: The Multi-Platform Environment for EGSnrc. Ionizing Radiation Standards, National Research Council of Canada, NRCC Report PIRS-877, 2006.
31. McGowan HC, Faddegon BA, Ma CM. STATDOSE for 3D Dose Distributions. Ionizing Radiation Standards, National Research Council of Canada, NRCC Report PIRS-0509(F), 2007.
32. Mijnheer B, Olszewska A, Fiorino C, Hartmann G, Knoos T, Rosenwald JC, *et al*. Quality Assurance of Treatment Planning Systems - Practical Examples for Non-IMRT Photon Beams. ESTRO Booklet No. 7, 2000.